Open access • Posted Content • DOI:10.1101/2020.01.15.907295

vRNA-vRNA interactions in influenza A virus HA vRNA packaging — **Source link**

Sho Miyamoto, Yukiko Muramoto, Keiko Shindo, Yoko Fujita ...+5 more authors

Institutions: Kyoto University

Related papers:

- Selective incorporation of influenza virus RNA segments into virions

- Identification of cis-acting packaging signals in the coding regions of the influenza B virus HA gene segment.

- The genome packaging signal of the influenza A virus genome comprises a genome incorporation signal and a genome bundling signal

- Structural and Functional Motifs in Influenza Virus RNAs.

- Heterologous influenza vRNA segments with identical non-coding sequences stimulate viral RNA replication in trans

1 **vRNA-vRNA interactions in influenza A virus HA vRNA**

2 **packaging**

3

4 Sho Miyamoto[1,2], Yukiko Muramoto[1], Keiko Shindo[1,3], Yoko Fujita[1,4],

5 Takeshi Morikawa[1,4], Ryoma Tamura[1,4], Jamie L Gilmore[1], Masahiro

6 Nakano[1,4], Takeshi Noda[1,4*]

7

8 [1] Laboratory of Ultrastructural Virology, Institute for Frontier Life and

9 Medical Sciences, Kyoto University, Kyoto, Japan

10 [2] Department of Molecular Virology, Graduate School of Medicine, Kyoto

11 University, Kyoto, Japan

12 [3] Keihanshin Consortium for Fostering the Next Generation of Global

13 Leaders in Research, Kyoto, Japan

14 [4] Laboratory of Ultrastructural Virology, Graduate School of Biostudies,

15 Kyoto University, Kyoto, Japan

16

17 * Corresponding author

18   E-mail: t-noda@infront.kyoto-u.ac.jp (TN)

19

Abstract

21 The genome of the influenza A virus is composed of eight single-stranded

22 negative-sense RNA segments (vRNAs). The eight different vRNAs are

23 selectively packaged into progeny virions. This process likely involves

24 specific interactions among vRNAs via segment-specific packaging signals

25 located in the 3' and 5' terminal coding regions of vRNAs. To identify

26 vRNA(s) that interact with hemagglutinin (HA) vRNA during genome

27 packaging, we generated a mutant virus, HA 5m2, which possessed five

28 silent mutations in the 5' packaging signal region of HA vRNA. The HA 5m2

29 virus had a specific defect in HA vRNA incorporation, which reduced the

30 viral replication efficiency. After serial passaging in cells, the virus acquired

31 additional mutations in the 5' terminal packaging signal regions of both HA

32 and PB2 vRNAs. These mutations contributed to recovery of viral growth

33 and packaging efficiency of HA vRNA. A direct RNA-RNA interaction

34 between the 5' ends of HA and PB2 vRNAs was confirmed *in vitro*. Our

35 results indicate that direct interactions of HA vRNA with PB2 vRNA via their

36 packaging signal regions are important for selective genome packaging and

3

37   enhance our knowledge on the emergence of pandemic influenza viruses

38   through genetic reassortment.

4

Introduction

40   The genome of the influenza A virus consists of eight segmented,

41 single-stranded, negative-sense viral RNAs (vRNAs). Each vRNA contains

42 a central coding region in an antisense orientation. This region is flanked

43 by segment-specific noncoding regions and common terminal promoter

44 sequences. Each vRNA forms a helical, rod-shaped ribonucleoprotein

45 complex (vRNP) that associates with multiple nucleoproteins (NPs) and with

46 a heterotrimeric RNA-dependent RNA polymerase complex composed of

47 PB2, PB1, and PA proteins. The vRNP is responsible for transcription and

48 replication of constituent vRNA. Recent studies examining NP-vRNA

49 interactions in the context of vRNPs have shown that the NPs bind to vRNA

50 nucleotides non-uniformly without sequence specificity[1, 2], suggesting

51 that some parts of the vRNAs are free of NPs, and can potentially form

52 secondary or tertiary structures that protrude from the surface of rod-

53 shaped vRNPs.

54   There is evidence to suggest that progeny virions selectively

55 package each copy of the eight vRNAs. In virions, the eight different vRNPs

5

56 are arranged in a specific '1+7' pattern, where one vRNP is surrounded by

57 the other seven vRNPs[3, 4]. The mechanism by which each copy of the

58 eight vRNAs is selected from a large pool of vRNAs and non-viral RNAs in

59 virus-infected cells, and how these vRNAs are organized into the specific

60 '1+7' arrangement, remains unclear. The segment-specific packaging signal

61 sequences, located in the noncoding and terminal coding regions of both

62 the 3' and 5' ends of each vRNA, likely ensure the integrity of genome

63 packaging[5-10]. The terminal coding regions within these packaging signal

64 sequences are thought to be involved in co-packaging of multiple vRNAs,

65 and are referred to as bundling signals [11]. Mutations or deletions in

66 bundling signal sequences reduce the packaging efficiency of several

67 vRNAs. The impact of such mutations or deletions on packaging efficiency

68 is hierarchical among the eight vRNAs[8, 12-19], suggesting that there are

69 specific interactions among the vRNPs. The vRNPs form sub-bundles *en*

70 *route* to the plasma membrane [20, 21], and vRNPs in virions are directly

71 or indirectly interconnected with each other[22, 23]; these findings offer

72 additional evidence for the existence of vRNA-vRNA interactions.

73   To further examine the likely involvement of vRNA-vRNA

74   interactions in genome packaging, it is necessary to identify which vRNA

75   segments interact with one another, and which regions of each vRNA

76   segment participate in these interactions. The potential *in-vitro* interactions

77   of various naked vRNA segments have previously been described in human

78   H3N2 and avian H5N2 viruses [22, 24]. However, the various combinations

79   of vRNA-vRNA interactions differ between the two viruses. It also remains

80   unclear whether such *in-vitro* vRNA-vRNA interactions in the absence of

81   NPs reflect interactions that may occur among vRNPs *in vivo*. Only some

82   nucleotides that are important for vRNA-vRNA interactions have been

83   identified in the context of virus replication in cells and co-packaging into

84   virions[22, 25]. These studies suggest that the 5' ends of M vRNA and the

85   central coding region of PB1 vRNA are involved in interactions and co-

86   packaging with NA vRNA, respectively. In addition, interactions between

87   PB1 and NS vRNAs may also be necessary for efficient viral replication and

88   genome packaging. However, the region in NS vRNA identified to interact

89   with PB1 vRNA is not located in the region of the previously reported

90   genome packaging signal [26]. Thus, the role of vRNA-vRNA interactions in

91   genome packaging remains unclear.

92   In this study, we used serial passaging to identify which vRNA(s)

93   interact with the hemagglutinin (HA) vRNA packaging signal in selective

94   genome packaging. We first generated a mutant influenza virus (A/WSN/33)

95   that possesses five silent mutations in the packaging signal of HA vRNA,

96   which causes a specific defect in the incorporation of HA vRNA. Then, we

97   serially passaged the mutant virus in cultured cells to restore efficient

98   incorporation of HA vRNA, and identified mutations that had been newly

99   introduced into the vRNAs. In addition, we examined the interactions of HA

100   vRNA with potential partner vRNAs *in vitro*, and assessed the importance

101   of these vRNA-vRNA interactions in the packaging signal regions specific

102   for HA vRNA incorporation and viral replication.

103

Results

Generation of mutant viruses possessing silent mutations in the packaging signal of HA vRNA.

We first disrupted the packaging signal sequence of HA vRNA which potentially interacts with other vRNAs during selective genome packaging. For this, we used reverse genetics to generate a series of mutant viruses that possessed five silent mutations in either the 3' or 5' packaging signal region of HA vRNA without any amino acid mutations (Fig 1A). The respective viral titers were examined by plaque assays (Fig 1B). Eight out of nine mutant viruses replicated at a level similar to that of the wild-type virus, showing titers of approximately 3.8×10^8 PFU/ml; however, an HA 5m2 virus, possessing five silent mutations at nucleotides 1664 to 1676 in HA vRNA, exhibited an approximately 87% reduced growth rate compared to the wild-type virus. Sequence analysis confirmed that no unexpected mutations occurred in any of the eight vRNAs of the HA 5m2 virus. These results indicate that nucleotides 1664 to 1674 in the packaging signal region of HA vRNA are necessary for efficient virus growth and are likely involved

9

121   in HA vRNA packaging, which in agreement with results reported by a

122   previous study[14].

123

124   **Serial passaging of the HA 5m2 virus in cells**

125   We hypothesized that after several passages, the HA 5m2 virus

126   would acquire adaptive mutations in vRNAs, which would restore viral

127   fitness. Accordingly, the HA 5m2 virus was serially passaged in Madin-

128   Darby Canine Kidney (MDCK) cells, and viral titers were assessed by

129   plaque assay after each passage. The viruses were designated as HA 5m2

130   P1, P2, P3, P4, P5, P6, P7, P8, P9, and P10 viruses, according to the

131   number of passages in MDCK cells. As expected, the growth of the HA 5m2

132   P10 virus was restored to approximately 61% of that shown by the wild-type

133   virus (Fig 2A). The titer of the HA 5m2 P10 virus did not increase with an

134   additional 10 passages (data not shown). Sequencing analysis of all eight

135   HA 5m2 P10 virus vRNAs revealed that two mutations were newly

136   introduced into the 5' terminal coding regions of HA vRNA (T1665C) and

137   PB2 vRNA (G2271T); both of these vRNAs are located within the previously

138   identified genome packaging signaling regions [6, 8, 14, 16].

139   To assess whether these two mutations contributed to the growth of

140   the HA 5m2 virus, we used reverse genetics to generate recombinant HA

141   5m2 viruses with additional mutation(s). Recombinant HA 5m2 viruses,

142   which possessed a single mutation in HA T1665C or PB2 G2271T, both

143   showed replication that was partially restored to 11 and 24% of the wild-

144   type virus, respectively (Fig 2B). The recombinant HA 5m2 virus with a

145   double mutation showed replication that was approximately 65% of the wild-

146   type virus, similar to the replication levels of the HA 5m2 P10 virus (Fig 2A

147   and 2B).

148   The HA T1665C and PB2 G2271T mutations lead to amino acid

149   substitutions HA S545P and PB2 Q748H, respectively. The amino acid 545

150   is located in the transmembrane region of the HA protein; hence, this

151   substitution may affect intracellular transport to the plasma membrane and

152   subsequent incorporation of HA proteins into progeny virions. Therefore, we

153   examined the amount of HA protein incorporated into progeny virions.

154   Western blotting showed that the amounts of HA protein were comparable

11

155   in the HA 5m2 P10, HA 5m2 P1, and wild-type virions. This suggests that

156   the S545P substitution has little or no effect on the amount of HA protein

157   incorporated into virions (Fig 2C). To examine the impact of the Q748H

158   substitution on the polymerase activity of the PB2 protein, we used RT-

159   qPCR to quantify the amount of vRNA in virus-infected cells at 7 hours post-

160   infection. The amount of vRNA was similar in HA 5m2 P10-infected, HA 5m2

161   P1-infected, and wild-type virus-infected cells, suggesting that the Q748H

162   substitution in PB2 had little or no effect on polymerase activity (Fig 2D).

163   Taken together, these results suggest that T1665C mutations in HA vRNA

164   and G2271T mutations in PB2 vRNA participate in the restoration of HA 5m2

165   viral replication at the RNA level.

166

167   **Efficiency of packaging eight vRNAs in HA 5m2 viruses**

168   Because the HA 5m2 virus possessed five silent mutations in the 5'

169   packaging signal region of HA vRNA, we predicted that it would show

170   defects in the packaging efficiency of vRNAs (especially of HA vRNA). We

171   also expected that additional mutations in the 5' packaging signals of HA

12

172   and PB2 vRNAs would improve the packaging efficiency of HA vRNA. To

173   assess the packaging efficiency of the HA 5m2 P1 and HA 5m2 P10 viruses,

174   we extracted vRNA from wild-type, HA 5m2 P1, and HA 5m2 P10 viruses;

175   then, we quantified the amount of the eight influenza vRNA segments using

176   RT-qPCR. As expected, the HA 5m2 P1 virus showed a marked defect in

177   the packaging efficiency of HA vRNA; the packaging efficiency was reduced

178   to approximately 24% compared with that of the wild-type virus. The HA 5m2

179   P1 virus also showed small defects in the packaging efficiency of PA, NP,

180   and NA vRNAs (Fig 3A). Importantly, in the HA 5m2 P10 virus, the packaging

181   efficiency of HA vRNA was largely recovered to approximately 72% of that

182   in the wild-type, and those of PA, NP, and NA vRNAs were also partially

183   recovered (Fig 3A).

184   To further examine the contribution of the PB2 G2271T and HA

185   T1665C mutations to vRNA packaging efficiency, we used RT-qPCR to

186   analyze the amount of packaged vRNA in recombinant HA 5m2 viruses

187   possessing a single mutation or a double mutation. In both recombinant HA

188   5m2 viruses with either a single PB2 G2271T or HA T1665C mutation, the

13

189   packaging efficiency of HA vRNA was restored to approximately 33 and 59%

190   to that of the wild-type virus, respectively (Fig 3B). In the recombinant HA

191   5m2 virus possessing the double mutation, the packaging efficiency of HA

192   vRNA was largely restored to approximately 77% of that of the wild-type

193   virus (Fig 3B); this was consistent with the packaging efficiency of HA vRNA

194   in the HA 5m2 P10 virus. Taken together, these results show that disruption

195   of the 5' genome packaging signal in HA vRNA reduces the packaging

196   efficiency of HA vRNA. Our results also show that additional mutations in

197   the sequences of 5' genome packaging signals of HA and PB2 vRNAs are

198   required for efficient HA vRNA packaging. This suggests that functional

199   interactions occur between HA and PB2 vRNAs via their 5' genome

200   packaging signals during viral replication.

201

202   **Ultrastructural analysis of the HA 5m2 viruses.**

203   To investigate how the RNPs are packaged into the HA 5m2 P1 and

204   HA 5m2 P10 viruses, we examined ultrathin sections via electron

205   microscopy (EM). Representative images of transversely and longitudinally

14

206   sectioned wild-type, HA 5m2 P1, and HA 5m2 P10 virions, budding from the

207   cell surfaces, are shown in Fig 4A. While some transversely sectioned wild-

208   type and HA 5m2 P10 virions appeared empty, as reported previously [26],

209   almost all longitudinally sectioned wild-type and HA 5m2 P10 virions

210   contained RNPs positioned at the tip of the budding virions. Conversely, the

211   HA 5m2 P1 viruses often possessed empty particles in both transverse and

212   longitudinal sections, suggesting that the HA 5m2 virus had defects in the

213   incorporation of RNPs.

214   To examine the incorporation of RNPs into virions in more detail,

215   we determined the proportion of empty particles in wild-type, HA 5m2 P1,

216   and HA 5m2 P10 viruses. For this, virions were purified by

217   ultracentrifugation through a sucrose cushion and observed by cryo-TEM

218   (Fig 4B). The particles of the wild-type virus mainly showed uniformly

219   spherical shapes of approximately 111 nm in diameter; 0.9% (n=1085) of

220   virions appeared empty or contained only a few vRNPs (Table 1). With a

221   diameter of approximately 87 nm (n=10, $p<0.0001$), such vRNP packaging-

222   deficient particles were significantly smaller than intact virions containing

15

223   multiple RNPs. The proportion of vRNP packaging-deficient particles in the

224   HA 5m2 P1 virus was 7.0% (n=1401), significantly higher than those of the

225   HA 5m2 P10 (3.2%, n=852, $p<0.0001$) and wild-type (0.9%, n=1085,

226      $p<0.0001$) viruses. The results of EM analysis support the notion that

227   potential interactions between the 5' packaging signals of HA and PB2

228   vRNAs are important for appropriate genome packaging.

229

Table 1. Effect of silent mutations and passages on the packaging of RNPs into progeny virions

	Experiment no.	wt	HA 5m2 P1	HA 5m2 P10
Proportion of vRNP packaging-deficient particles	1	3 / 341 (0.9%)	32 / 505 (6.3%)	14 / 370 (3.7%)
	2	7 / 744 (0.9%)	66 / 896 (7.4%)	13 / 482 (2.7%)
	Total	10 / 1085 (0.9%)	98 / 1401 (7.0%)	27 / 852 (3.2%)
p-value*		<0.0001		<0.0001

230   *Proportions of vRNP packaging-deficient particles in each virus were

231   compared with that in the HA 5m2 P1 virus. Data were analyzed using

232   Dunnett's test.

233

16

234   **A direct interaction between HA and PB2 vRNA occurs via the 5' ends**

235   **of packaging signals *in vitro***

236   We next aimed to confirm that a functional interaction between the

237   5' terminal regions of HA and PB2 vRNAs is involved in efficient packaging

238   of HA vRNA. For this, we used a gel shift assay to examine whether direct

239   RNA-RNA interactions between these two vRNAs occur *in vitro*. To eliminate

240   possible nonspecific interactions via the non-packaging signal regions of

241   vRNAs, we synthesized a short HA vRNA comprising the 5' noncoding

242   region and the 120-nucleotide long coding region, which is designated as

243   5'HA(120). We also synthesized a short PB2 vRNA comprising the 5'

244   noncoding region and the 300-nucleotide long coding region, which is

245   designated as 5'PB2(300) (Fig 5A). In addition to the 5'HA(120) possessing

246   the wild-type HA vRNA sequence, we synthesized mutant 5'HA(120)

247   sequences into which we introduced five silent mutations corresponding to

248   HA 5m1, HA 5m2, HA 5m3, HA 5m4, and HA 5m5 (Fig 1A); these mutant

249   5'HA(120) vRNAs were designated as 5'HA(120) 5m1, 5'HA(120) 5m2,

250   5'HA(120) 5m3, 5'HA(120) 5m4, and 5'HA(120) 5m5, respectively. The

17

251   mixture of wild-type 5'HA(120) and 5'PB2(300) showed slower migration of

252   the band, indicating formation of a vRNA-vRNA complex (Figs 5B and 5C).

253   The mutant 5'HA(120) 5m1, 5'HA(120) 5m3, 5'HA(120) 5m4, and 5'HA(120)

254   5m5 vRNAs also formed a complex with 5'PB2(300), whose proportions

255   were 69-95% compared to the complex of 5'HA(120) and 5'PB2(300). These

256   results are consistent with our viral replication data, showing that such

257   mutations in HA vRNA did not markedly affect viral growth (Fig 1B). In

258   contrast, the 5'HA(120) 5m2 vRNA associated with 5'PB2(300) to a lesser

259   degree and did not form a vRNA-vRNA complex efficiently, with only 12%

260   complex formation compared to the 5'HA(120) and 5'PB2(300), correlating

261   with the reduced viral growth of the HA 5m2 virus (Fig 1B). Taken together,

262   these results indicate that there is an interaction between the 5' packaging

263   signals of HA and PB2 vRNAs in the context of vRNPs, which is important

264   for optimal packaging of HA vRNA.

265

Discussion

266

267   Specific interactions among eight different vRNAs are likely

268   required for selective genome packaging of the influenza viruses. To identify

269   the interactions of HA vRNA in the context of RNPs, we generated a mutant

270   HA 5m2 virus with reduced packaging efficiency of HA vRNA, and repeatedly

271   passaged this virus in cultured cells to restore viral fitness. We found that

272   the HA 5m2 virus acquired additional mutations in the 5' packaging signal

273   sequences of HA and PB2 vRNAs; this restored HA vRNA packaging

274   efficiency and viral growth. Our results suggest that the packaging signal at

275   the 5' terminal coding region of HA vRNA is involved in co-packaging of the

276   eight different vRNAs; this likely occurs via a direct RNA-RNA interaction

277   with the 5' packaging signal of PB2 vRNA. To the best of our knowledge,

278   this is the first study experimentally showing that a packaging-deficient

279   virus can recover its packaging efficiency by the introduction of mutations

280   in other vRNA segments during viral replication.

281   The 5' packaging signal sequence, located at nucleotides 1662 to

282   1681 in HA vRNA, is more than 90% conserved in H1 subtype influenza

19

283   viruses. However, the neighboring regions show less sequence

284   conservation [14], suggesting that this region is important for HA vRNA

285   packaging at the RNA level. Our results show that introduction of five silent

286   mutations into the highly conserved region at nucleotides 1664 to 1676 in

287   HA vRNA reduced the incorporation efficiency of HA vRNA (Fig. 2A). An

288   additional mutation at nucleotide 1665 restored the reduced efficiency of

289   HA vRNA packaging (Fig. 2B). This confirms that the highly conserved

290   region in the sequence of the 5' terminal packaging signal is involved in

291   incorporation of HA vRNA. Recent findings indicate that NP non-uniformly

292   decorates vRNA [1, 2]. Therefore, it is possible that the region at

293   nucleotides 1664 to 1676 in HA vRNA, identified in this study, is NP-free

294   and forms secondary or tertiary structures on vRNPs to interact with the 5'

295   packaging signal of PB2 vRNA. However, whether the 5' terminal coding

296   region of HA vRNA is a low NP-binding region remains unclear [1, 2].

297   Additional work is necessary to determine the precise location of the NP-

298   free region of HA vRNA in the A/WSN/33 strain.

299   After the HA 5m2 virus was serially passaged in MDCK cells, the

20

300   virus acquired a G2271T mutation in the 5' packaging signal sequence of

301   PB2 vRNA, which recovered the reduced incorporation of HA vRNA (Fig.

302   2B). This finding suggests that the region around nucleotide 2271 in PB2

303   vRNA is involved in interactions with HA vRNA. However, a previous study

304   showed that the introduction of silent mutations at nucleotides 2268 to 2286,

305   including a mutation at nucleotide 2271, in PB2 vRNA did not reduce the

306   packaging efficiency of HA vRNA [14]. Therefore, it is possible that the

307   mutation at G2271T in PB2 vRNA, found in this study, was acquired for the

308   optimal packaging of HA 5m2 vRNA but not of wild-type HA vRNA.

309   Although the 5' terminal coding region of H1 subtype HA vRNA is

310   conserved in H1 HA vRNA, it is substantially different from other subtypes

311   of HA vRNAs at the nucleotide level [13]. In contrast, the 5' terminal coding

312   region of PB2 vRNA is highly conserved in influenza viruses [13, 17],

313   suggesting that intersegmental interactions between HA and PB2 vRNAs

314   via their 5' terminal regions may be specific to the H1 subtype. Native gel

315   electrophoresis analysis of *in-vitro* vRNA-vRNA interactions revealed that

316   avian H5N2 and human H3N2 viruses show different intersegmental

21

317   networks among the eight vRNAs, and do not show strong interactions

318   between HA and PB2 vRNAs [22, 24]. In the context of vRNPs, *in-vitro*

319   interactions do not necessarily reflect interactions *in-vivo*. Therefore,

320   further studies are needed to clarify whether HA vRNAs of other subtypes

321   require interactions with PB2 vRNA for HA vRNA packaging in the context

322   of vRNPs.

323   The reduced HA vRNA packaging efficiency of the HA 5m2 virus was

324   rescued when the virus spontaneously acquired adaptive mutations in HA

325   and PB2 vRNAs during serial passaging (Fig. 2A and 2B). Previously, Marsh

326   et al., serially passaged an influenza A virus (WSN strain), which possesses

327   synonymous mutations in HA vRNAs, to determine whether the virus would

328   generate adaptive mutations for recovery of the reduced HA vRNA

329   packaging efficiency. However, the virus did not generate any mutations to

330   improve viral fitness [14]. This may have been due to the number of

331   synonymous mutations introduced into the HA vRNAs. Nine nucleotide

332   mutations were introduced into the region of 1659 to 1673 in the HA vRNAs

333   in the study by Marsh et al., while only five mutations were introduced into

334   the region of 1664 to 1679 in HA vRNAs in our present study. More

335   mutations may cause severe incompatibility in vRNA-vRNA interactions.

336   Even repeated serial passaging may not generate multiple nucleotide

337   changes in HA vRNA and its respective interacting vRNA to restore the HA

338   vRNA packaging efficiency.

339   In conclusion, we have shown that an interaction between HA vRNA

340   and PB2 vRNA via the 5' packaging signals is important for HA vRNA

341   packaging. Our results suggest that HA vRNA is co-packaged with PB2

342   vRNA into virions. These findings will help us understand how reassortant

343   influenza viruses incorporate HA vRNA segments, and how pandemic

344   viruses emerge via genetic reassortment.

345

Materials and Methods

Cells

Human embryonic kidney (293T) cells were maintained in Dulbecco's Modified Eagle Medium (D6046, Sigma) supplemented with 10% fetal bovine serum (FB-1365, Biosera, Chile). Madin-Darby Canine Kidney (MDCK) cells were grown in Minimal Essential Medium (MEM)(11430-030, Gibco) containing 5% newborn calf serum (16010-159, Gibco, New Zealand). Cultures were maintained at 37°C in a 5% CO_2 atmosphere. The medium used during viral infection of cells was MEM containing 0.3% bovine serum albumin (BSA/MEM).

Construction of the PolI HA plasmid

To generate the PolI HA mutant plasmid, we amplified the PolI-HA plasmid by inverse PCR using a previously published protocol [27]. The primers used are listed in S1 Table.

Reverse genetics

24

363   Reverse genetics were performed using PolI plasmids that

364   contained cDNA sequences of the A/WSN/33(H1N1) viral genes; all

365   procedures were conducted as described previously [28]. Briefly, eight PolI

366   plasmids and pCAGGS protein-expression plasmids for PB2, PB1, PA, and

367   NP were mixed with the transfection reagent TransIT-293 (Mirus), and

368   added to 293T cells cultured in BSA/MEM. At 48 hours post-transfection,

369   the cells were treated with 1 µg /ml of TPCK-Trypsin for 30 min, centrifuged

370   at 1750 × g for 15 min at 4ºC, and the supernatant was harvested and stored

371   at -80ºC. To generate mutant viruses, the PolI-HA wt plasmid was replaced

372   with a PolI-HA mutant plasmid. Viral titers were determined by a plaque

373   assay conducted using MDCK cells.

374

375   **Virus purification**

376   After collecting the supernatants from virus-infected MDCK cells,

377   each supernatant was clarified by centrifugation at 1750 × g for 15 min at

378   4ºC, followed by another centrifugation at 6700 × g for 30 min at 4ºC. To

379   eliminate RNAs outside of the virus particles, the supernatants were treated

25

380   with 5 µg/ml RNase A (Nacalai Tesque) for 1 hour at 37°C. Virions in the

381   supernatants were purified by ultracentrifugation through a 30% (w/w)

382   sucrose cushion at 125,000 × g for 2 hours at 4°C. The pellets were then

383   resuspended in phosphate buffered saline (PBS).

384

385   **Western blotting**

386   MDCK cells were infected with the viruses at a multiplicity of

387   infection (MOI) of 1 on ice for 1 hour. The infected MDCK cells were then

388   cultured in BSA/MEM containing 1 µg /ml TPCK-Trypsin. At 10 hours post-

389   infection, the supernatant was harvested and purified as described above.

390   The purified virus was dissolved with an equal volume of 2x Tris-Glycine

391   SDS Sample Buffer (Thermo Fisher Scientific) and boiled for 5 min without

392   a reducing agent, and then subjected to SDS-PAGE. Proteins were

393   electroblotted onto Immobilon-P transfer membranes (Millipore

394   Corporation). The membranes were blocked with Blocking One (Nacalai

395   Tesque) for 30 min at room temperature, and then incubated with goat anti-

396   influenza A virus polyclonal antibody (ab20841, Abcam, 1:10,000 dilution)

397   overnight at 4°C. After incubation with rabbit anti-goat IgG secondary

398   antibody (ab6741, Abcam, 1:10,000 dilution) for 1 hour at room temperature,

399   the blots were developed using a Chemi-Lumi One Super (Nacalai Tesque).

400

401   **RT-qPCR**

402   The packaged vRNAs were extracted from purified viruses using an

403   RNeasy Mini Kit (Qiagen). 100 ng of extracted vRNAs were reverse

404   transcribed using a Uni-12 primer (5'-AGCRAAAGCAGG-3') and

405   Superscript III reverse transcriptase (Invitrogen). Quantification was

406   performed by qPCR on a Rotor-Gene Q 2plex System (Qiagen) using

407   segment-specific primers modified from the protocol by Marsh *et al*. The

408   primers used are listed in S1 Table. For each sample, reactions contained

409   1 µl 10-fold diluted RT product, 7.5 µl THUNDERBIRD SYBR qPCR Mix

410   (Toyobo), 0.25 µM segment-specific primers, for a final volume of 15 µl.

411   Cycling conditions were: 2 min at 94°C, followed by 40 cycles (98°C for 10

412   s, 55°C for 15 s, and 72°C for 30 s).

413   In Figure 2D, total RNA was extracted from virus-infected cells

27

414   using an RNeasy Mini Kit (Qiagen). For PB2, PB1, HA, and NP vRNAs, RT-

415   qPCR was performed as described above, using 100 ng total RNA. The

416   values were expressed as numbers of RNA copies in an infected cell,

417   assuming that a cell contained 10 pg of RNA [29, 30].

418

419   **Ultrathin section electron microscopy (EM)**

420   Ultrathin section EM was performed as described previously [3].

421   MDCK cells were infected at MOI=10. At 10 hours post-infection, the

422   infected cells were prefixed with 2.5% glutaraldehyde in 0.1 M cacodylate

423   buffer (pH 7.4) on ice. Ultrathin (50-nm-thick) sections were stained with 2%

424   uranyl acetate in 70% ethanol and in Reynold's lead citrate. Representative

425   images were acquired using HT7700 (Hitachi).

426

427   **Quantification of vRNP packaging-deficient particles**

428   Purified viruses were applied onto C-flat holey carbon grids

429   (Protichips), which were blotted on a Vitrobot Mark IV (Thermo Fisher

430   Scientific) before plunge-freezing in liquid ethane. Samples were kept cool

431   in liquid nitrogen. Samples were imaged at 200 kV on a Talos F200C

432   (Thermo Fisher Scientific) equipped with a Ceta 16M CMOS camera (Gatan).

433   More than 300 particles were observed for each experiment.

434

435   *In vitro* **RNA synthesis**

436   Shortened HA and PB2 vRNAs were synthesized *in vitro* using T7

437   transcription as described previously [30]. Briefly, templates containing a

438   T7 phage promoter sequence (5'-TAATACGACTCACTATAGGG-3') were

439   amplified by PCR using corresponding primer pairs and were purified with

440   a QIAquick PCR purification kit (Qiagen). The primers used are listed in S1

441   Table. Purified PCR products were transcribed *in vitro* using the RiboMAX

442   Large Scale RNA Production System-T7 (Promega) at 37°C for 4 h, followed

443   by RQ1 DNase I (Promega) digestion of the DNA template at 37°C for 15

444   min. The transcript was purified with an RNeasy Mini Kit.

445

446   **RNA binding assay**

447   RNA-RNA interactions were analyzed by electrophoretic mobility

448   shift assays essentially as described previously [24]. To facilitate RNA

449   folding, adjustments were made to the reaction buffer employed and

450   incubation time as described below [31]. Pairs of purified vRNAs (2 pmol of

451   each vRNA) were denatured for 10 min at 65°C in 5 µl of ultrapure water

452   and cooled on ice. We then added 5 µl of 2-fold concentrated buffer (final

453   concentration: 50 mM HEPES, 50 mM KCl, and 20 mM $MgCl_2$) and incubated

454   the samples for 2 hours at 37°C. Then, 2 µl of loading buffer [40% (v/v)

455   glycerol and 0.05% (w/v) bromophenol blue] was added to the samples, and

456   the samples were analyzed using 1.0% agarose gels containing 0.01% (w/v)

457   ethidium bromide. Native gel electrophoresis of the RNA complexes was

458   performed at 4°C in a buffer containing 50 mM Tris, 44.5 mM borate, and

459   0.1 mM $MgCl_2$. We then determined the RNA weight fraction (%) of each

460   band in each lane. The percentage of intermolecular complex formation was

461   determined by dividing the weight fraction of a band by the sum of weight

462   fractions in the corresponding lane.

463

464   **Statistical analysis**

465   The statistical significance of the viral titers, the proportions of

466   vRNP packaging-deficient particles and the formation efficiencies of vRNA-

467   vRNA complexes were calculated using Dunnett's test. Diameters of virus

468   particles observed by EM were statistically analyzed using Welch's t-test. P

469   values of < 0.01 were considered significant.

470

471 **Acknowledgments**

472 We thank Connor Park for editing the manuscript.

473

References

474

475   1.   Williams GD, Townsend D, Wylie KM, Kim PJ, Amarasinghe GK,

476   Kutluay SB, et al. Nucleotide resolution mapping of influenza A virus

477   nucleoprotein-RNA interactions reveals RNA features required for

478   replication. Nature communications. 2018;9(1):465. Epub 2018/02/02. doi:

479   10.1038/s41467-018-02886-w. PubMed PMID: 29386621; PubMed Central

480   PMCID: PMCPMC5792457.

481   2.   Lee N, Le Sage V, Nanni AV, Snyder DJ, Cooper VS, Lakdawala SS.

482   Genome-wide analysis of influenza viral RNA and nucleoprotein association.

483   Nucleic acids research. 2017;45(15):8968-77. doi: 10.1093/nar/gkx584.

484   3.   Noda T, Sagara H, Yen A, Takada A, Kida H, Cheng RH, et al.

485   Architecture of ribonucleoprotein complexes in influenza A virus particles.

486   Nature.   2006;439(7075):490-2.   Epub   2006/01/27.   doi:

487   10.1038/nature04378. PubMed PMID: 16437116.

488   4.   Chou YY, Vafabakhsh R, Doganay S, Gao Q, Ha T, Palese P. One

489   influenza virus particle packages eight unique viral RNAs as shown by FISH

490   analysis. Proceedings of the National Academy of Sciences of the United

491   States of America. 2012;109(23):9101-6. Epub 2012/05/02. doi:

492   10.1073/pnas.1206069109. PubMed PMID: 22547828; PubMed Central

493   PMCID: PMCPMC3384215.

494   5.   Fujii Y, Goto H, Watanabe T, Yoshida T, Kawaoka Y. Selective

495   incorporation of influenza virus RNA segments into virions. Proceedings of

496   the National Academy of Sciences of the United States of America.

497   2003;100(4):2002-7. Epub 2003/02/08. doi: 10.1073/pnas.0437772100.

498   PubMed PMID: 12574509; PubMed Central PMCID: PMCPMC149948.

499   6.   Watanabe T, Watanabe S, Noda T, Fujii Y, Kawaoka Y. Exploitation

500   of nucleic acid packaging signals to generate a novel influenza virus-based

501   vector stably expressing two foreign genes. Journal of virology.

502   2003;77(19):10575-83. Epub 2003/09/13. PubMed PMID: 12970442;

503   PubMed Central PMCID: PMCPMC228515.

504   7.   Fujii K, Fujii Y, Noda T, Muramoto Y, Watanabe T, Takada A, et al.

505   Importance of both the coding and the segment-specific noncoding regions

506   of the influenza A virus NS segment for its efficient incorporation into virions.

507   Journal of virology. 2005;79(6):3766-74. Epub 2005/02/26. doi:

508   10.1128/jvi.79.6.3766-3774.2005. PubMed PMID: 15731270; PubMed

509   Central PMCID: PMCPMC1075679.

510   8.   Muramoto Y, Takada A, Fujii K, Noda T, Iwatsuki-Horimoto K,

511   Watanabe S, et al. Hierarchy among viral RNA (vRNA) segments in their

512   role in vRNA incorporation into influenza A virions. Journal of virology.

513   2006;80(5):2318-25. Epub 2006/02/14. doi: 10.1128/jvi.80.5.2318-

514   2325.2006. PubMed PMID: 16474138; PubMed Central PMCID:

515   PMCPMC1395381.

516   9.   Ozawa M, Fujii K, Muramoto Y, Yamada S, Yamayoshi S, Takada A,

517   et al. Contributions of two nuclear localization signals of influenza A virus

518   nucleoprotein to viral replication. Journal of virology. 2007;81(1):30-41.

519   Epub 2006/10/20. doi: 10.1128/jvi.01434-06. PubMed PMID: 17050598;

520   PubMed Central PMCID: PMCPMC1797272.

521   10.   Ozawa M, Maeda J, Iwatsuki-Horimoto K, Watanabe S, Goto H,

522   Horimoto T, et al. Nucleotide sequence requirements at the 5' end of the

523   influenza A virus M RNA segment for efficient virus replication. Journal of

524   virology. 2009;83(7):3384-8. Epub 2009/01/23. doi: 10.1128/jvi.02513-08.

525   PubMed PMID: 19158245; PubMed Central PMCID: PMCPMC2655591.

526   11.   Goto H, Muramoto Y, Noda T, Kawaoka Y. The genome-packaging

527   signal of the influenza A virus genome comprises a genome incorporation

528   signal   and   a   genome-bundling   signal.   Journal   of   virology.

529   2013;87(21):11316-22.   Epub   2013/08/09.   doi: 10.1128/jvi.01301-13.

530   PubMed PMID: 23926345; PubMed Central PMCID: PMCPMC3807325.

531   12.   Liang Y, Hong Y, Parslow TG. cis-Acting packaging signals in the

532   influenza virus PB1, PB2, and PA genomic RNA segments. Journal of

533   virology.   2005;79(16):10348-55.   Epub   2005/07/30.   doi:

534   10.1128/jvi.79.16.10348-10355.2005. PubMed PMID: 16051827; PubMed

535   Central PMCID: PMCPMC1182667.

536   13.   Gog JR, Afonso Edos S, Dalton RM, Leclercq I, Tiley L, Elton D, et

537   al. Codon conservation in the influenza A virus genome defines RNA

538   packaging signals. Nucleic acids research. 2007;35(6):1897-907. Epub

539   2007/03/03. doi: 10.1093/nar/gkm087. PubMed PMID: 17332012; PubMed

540   Central PMCID: PMCPMC1874621.

541   14.   Marsh GA, Hatami R, Palese P. Specific residues of the influenza A

542   virus hemagglutinin viral RNA are important for efficient packaging into

543   budding virions. Journal of virology. 2007;81(18):9727-36. Epub 2007/07/20.

544   doi: 10.1128/jvi.01144-07. PubMed PMID: 17634232; PubMed Central

545   PMCID: PMCPMC2045411.

546   15.   Hutchinson EC, Curran MD, Read EK, Gog JR, Digard P. Mutational

547   analysis of cis-acting RNA signals in segment 7 of influenza A virus. Journal

548   of   virology.   2008;82(23):11869-79.   Epub   2008/09/26.   doi:

549   10.1128/jvi.01634-08. PubMed PMID: 18815307; PubMed Central PMCID:

550   PMCPMC2583641.

551   16.   Liang Y, Huang T, Ly H, Parslow TG, Liang Y. Mutational analyses

552   of packaging signals in influenza virus PA, PB1, and PB2 genomic RNA

553   segments. Journal of virology. 2008;82(1):229-36. Epub 2007/10/26. doi:

554   10.1128/jvi.01541-07. PubMed PMID: 17959657; PubMed Central PMCID:

555   PMCPMC2224372.

556   17.   Marsh GA, Rabadan R, Levine AJ, Palese P. Highly conserved

557   regions of influenza a virus polymerase gene segments are critical for

558   efficient viral RNA packaging. Journal of virology. 2008;82(5):2295-304.

559   Epub 2007/12/21. doi: 10.1128/jvi.02267-07. PubMed PMID: 18094182;

560   PubMed Central PMCID: PMCPMC2258914.

561   18.   Hutchinson EC, Wise HM, Kudryavtseva K, Curran MD, Digard P.

562   Characterisation of influenza A viruses with mutations in segment 5

563   packaging signals. Vaccine. 2009;27(45):6270-5. Epub 2009/10/21. doi:

564   10.1016/j.vaccine.2009.05.053. PubMed PMID: 19840659; PubMed Central

565   PMCID: PMCPMC2771075.

566   19.   Gao Q, Chou YY, Doganay S, Vafabakhsh R, Ha T, Palese P. The

567   influenza A virus PB2, PA, NP, and M segments play a pivotal role during

568   genome packaging. Journal of virology. 2012;86(13):7043-51. Epub

569   2012/04/26. doi: 10.1128/jvi.00662-12. PubMed PMID: 22532680; PubMed

570   Central PMCID: PMCPMC3416350.

571   20.   Chou YY, Heaton NS, Gao Q, Palese P, Singer RH, Lionnet T.

572   Colocalization of different influenza viral RNA segments in the cytoplasm

573   before viral budding as shown by single-molecule sensitivity FISH analysis.

574   PLoS   pathogens.   2013;9(5):e1003358.   Epub   2013/05/15.   doi:

575   10.1371/journal.ppat.1003358. PubMed PMID: 23671419; PubMed Central

576   PMCID: PMCPMC3649991.

577   21.   Lakdawala SS, Wu Y, Wawrzusin P, Kabat J, Broadbent AJ,

578   Lamirande EW, et al. Influenza a virus assembly intermediates fuse in the

579   cytoplasm. PLoS pathogens. 2014;10(3):e1003971. Epub 2014/03/08. doi:

580   10.1371/journal.ppat.1003971. PubMed PMID: 24603687; PubMed Central

581   PMCID: PMCPMC3946384.

582   22.   Fournier E, Moules V, Essere B, Paillart JC, Sirbat JD, Isel C, et al.

583   A supramolecular assembly formed by influenza A virus genomic RNA

584   segments. Nucleic acids research. 2012;40(5):2197-209. Epub 2011/11/15.

585   doi: 10.1093/nar/gkr985. PubMed PMID: 22075989; PubMed Central

586   PMCID: PMCPMC3300030.

587   23.   Noda T, Sugita Y, Aoyama K, Hirase A, Kawakami E, Miyazawa A,

588   et al. Three-dimensional analysis of ribonucleoprotein complexes in

589   influenza A virus. Nature communications. 2012;3:639. Epub 2012/01/26.

590   doi: 10.1038/ncomms1647. PubMed PMID: 22273677; PubMed Central

591   PMCID: PMCPMC3272569.

592   24.   Gavazzi C, Isel C, Fournier E, Moules V, Cavalier A, Thomas D, et

593   al. An in vitro network of intermolecular interactions between viral RNA

594   segments of an avian H5N2 influenza A virus: comparison with a human

595   H3N2 virus. Nucleic acids research. 2013;41(2):1241-54. Epub 2012/12/12.

596   doi: 10.1093/nar/gks1181. PubMed PMID: 23221636; PubMed Central

597   PMCID: PMCPMC3553942.

598   25.   Gilbertson B, Zheng T, Gerber M, Printz-Schweigert A, Ong C,

599   Marquet R, et al. Influenza NA and PB1 Gene Segments Interact during the

600   Formation of Viral Progeny: Localization of the Binding Region within the

601   PB1 Gene. Viruses. 2016;8(8). Epub 2016/08/25. doi: 10.3390/v8080238.

602   PubMed PMID: 27556479; PubMed Central PMCID: PMCPMC4997600.

603   26.   Gavazzi C, Yver M, Isel C, Smyth RP, Rosa-Calatrava M, Lina B, et

604   al. A functional sequence-specific interaction between influenza A virus

605   genomic RNA segments. Proceedings of the National Academy of Sciences

606   of the United States of America. 2013;110(41):16604-9. Epub 2013/09/27.

607   doi: 10.1073/pnas.1314419110. PubMed PMID: 24067651; PubMed Central

608   PMCID: PMCPMC3799358.

609   27.   Ochman H, Gerber AS, Hartl DL. Genetic applications of an inverse

610   polymerase chain reaction. Genetics. 1988;120(3):621-3. Epub 1988/11/01.

611   PubMed PMID: 2852134; PubMed Central PMCID: PMCPMC1203539.

612   28.   Neumann G, Watanabe T, Ito H, Watanabe S, Goto H, Gao P, et al.

613   Generation of influenza A viruses entirely from cloned cDNAs. Proceedings

614   of the National Academy of Sciences of the United States of America.

615   1999;96(16):9345-50. Epub 1999/08/04. PubMed PMID: 10430945; PubMed

616   Central PMCID: PMCPMC17785.

617   29.   Hatada E, Hasegawa M, Mukaigawa J, Shimizu K, Fukuda R.

618   Control of Influenza Virus Gene Expression: Quantitative Analysis of Each

619   Viral RNA Species in Infected Cells. The Journal of Biochemistry.

620   1989;105(4):537-46.

621   30.   Kawakami E, Watanabe T, Fujii K, Goto H, Watanabe S, Noda T, et

622   al. Strand-specific real-time RT-PCR for distinguishing influenza vRNA,

623   cRNA, and mRNA. Journal of virological methods. 2011;173(1):1-6. Epub

624   2010/12/28. doi: 10.1016/j.jviromet.2010.12.014. PubMed PMID: 21185869;

625   PubMed Central PMCID: PMCPMC3049850.

626   31.   Buchmueller KL, Weeks KM. Tris-borate is a poor counterion for

627   RNA: a cautionary tale for RNA folding studies. Nucleic acids research.

628   2004;32(22):e184. Epub 2004/12/17. doi: 10.1093/nar/gnh182. PubMed

629   PMID: 15601995; PubMed Central PMCID: PMCPMC545480.

630

A.
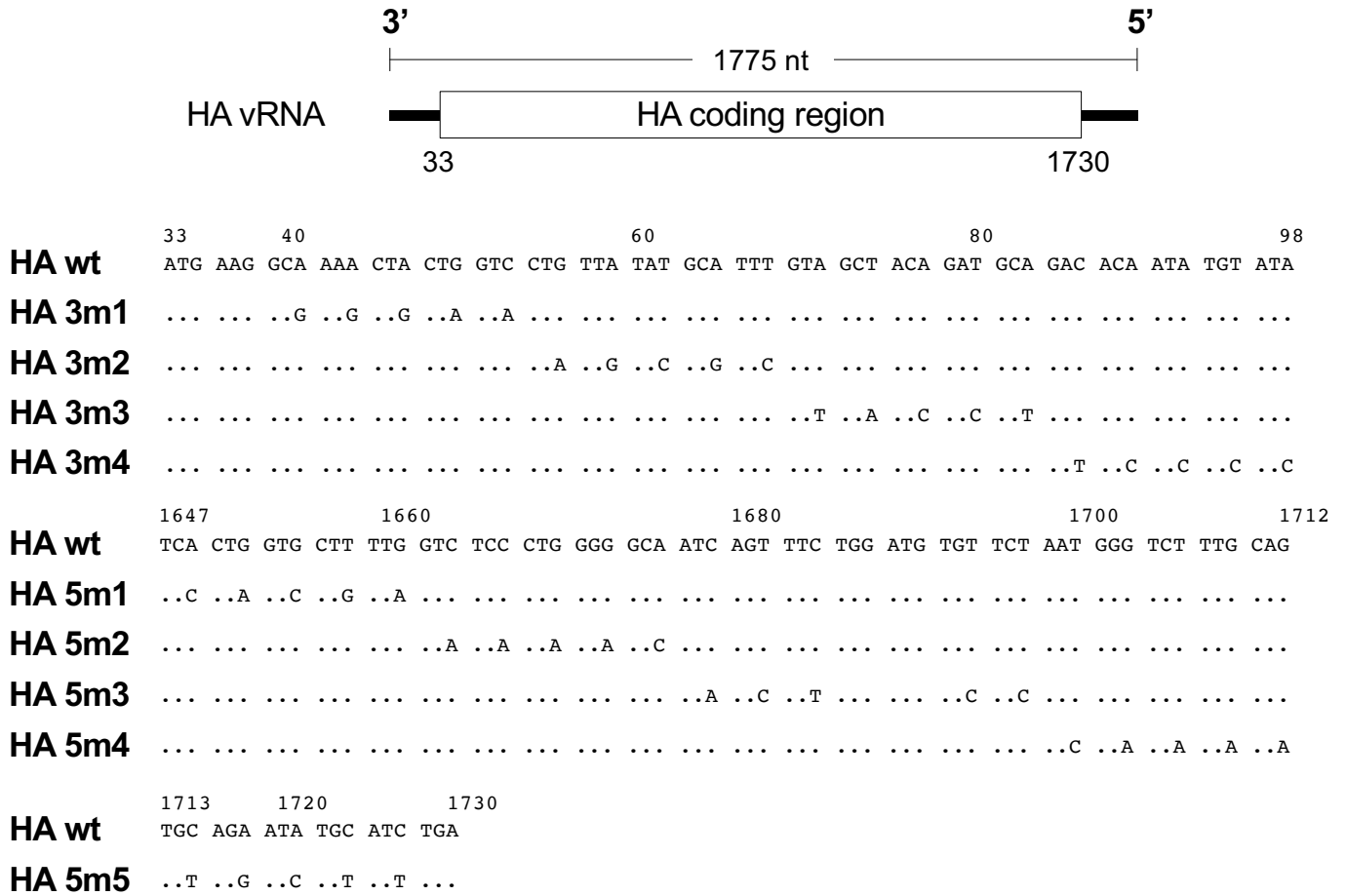
B.
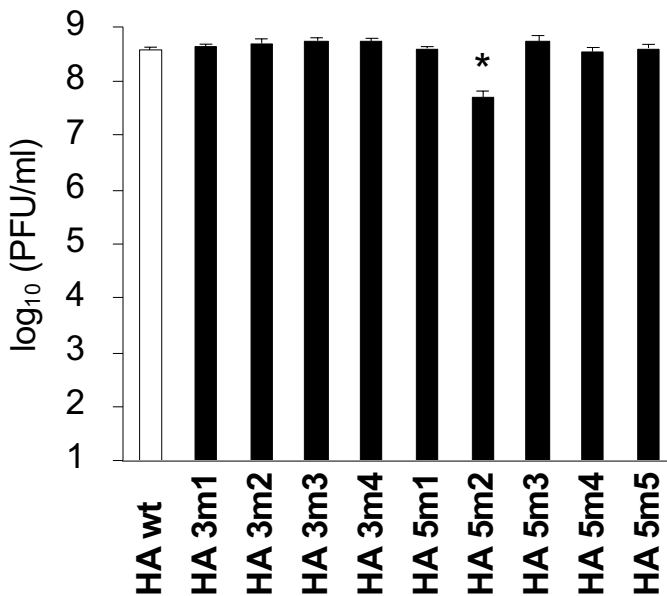
Fig 1. Generation of mutant influenza A viruses by reverse genetics and replication efficiencies of these mutant viruses. (A) Schematic diagram of mutant HA vRNAs with silent mutations introduced into the packaging signal sequences. The 3' and 5' ends of the HA coding region (nucleotides 33–98 and 1649–1730, respectively) are shown in the mRNA-sense orientation. (B) 293T cells were transfected with plasmids to produce the mutant and wild-type viruses. MDCK cells were infected with these mutant and wild-type viruses at a multiplicity of infection (MOI) of 10^{-5}. Virus yields at 48 h post-infection were determined by a plaque assay on MDCK cells. The data represent the mean ± SD (n = 3). Dunnett's test; *P < 0.01

Figure 1
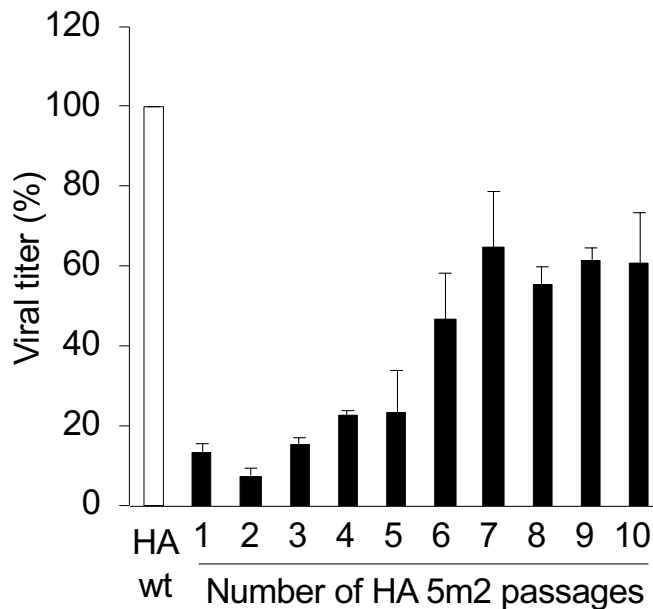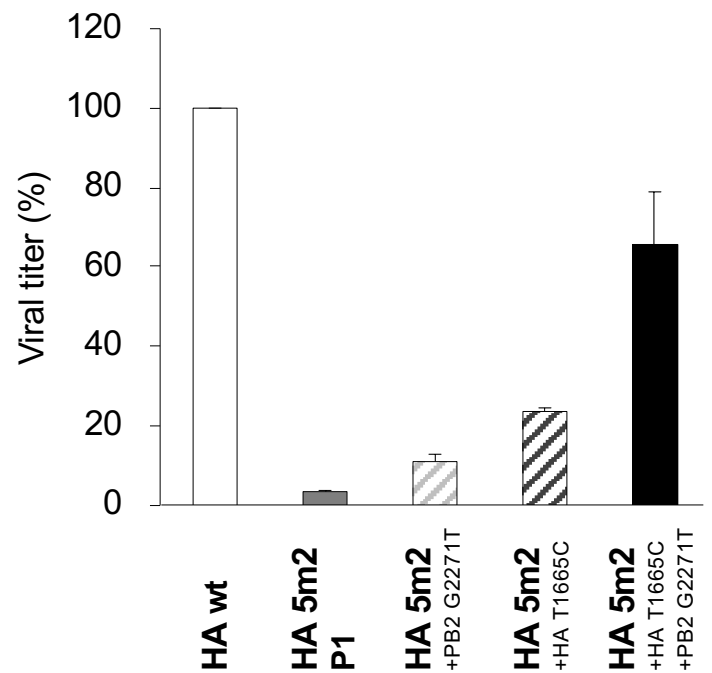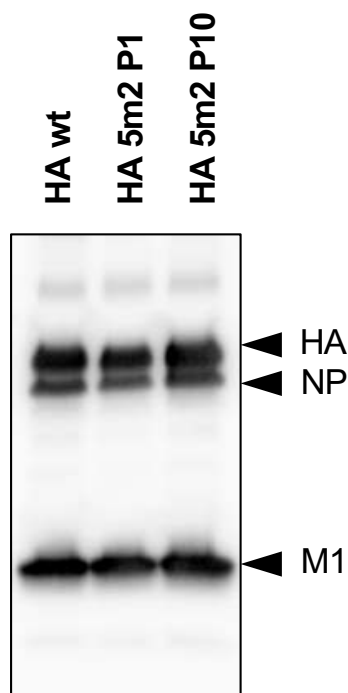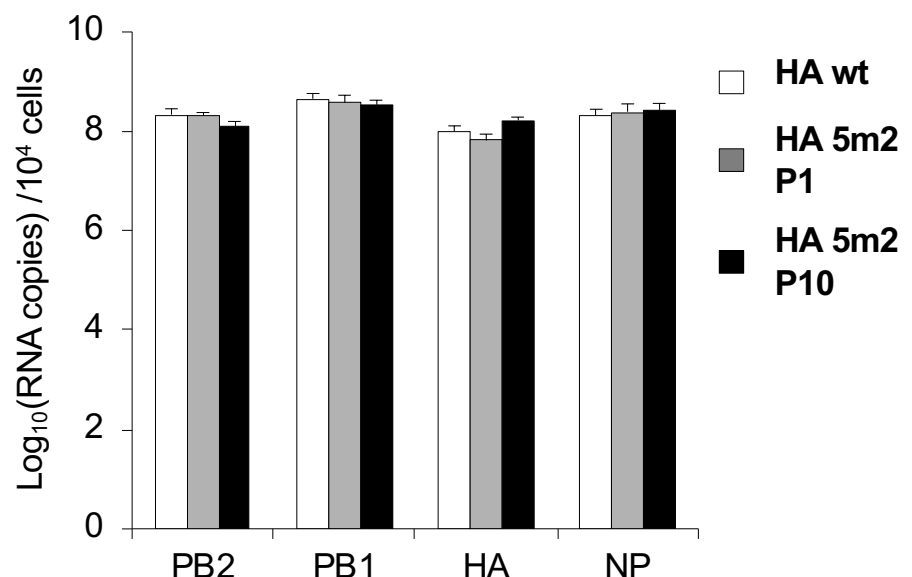
Fig 2. Analysis of HA 5m2 viral replication. (A) The HA 5m2 virus was passaged in MDCK cells at an MOI of 10^{-5}. For each passage, supernatants were collected at 48 hours post-infection, and viral yields were determined by a plaque assay on MDCK cells. (B) 293T cells were transfected with plasmids to produce the mutant HA5m2 and wild-type viruses. After infecting MDCK cells at an MOI of 10^{-5}, viral yields were determined at 48 hours post-infection. The data represent the mean ± SD (n = 3). (C) The purified viruses were analyzed via western blot using an anti-influenza A virus polyclonal antibody against HA, NP, and M1. (D) MDCK cells were infected with the viruses at an MOI of 1. Total RNA was extracted at 7 hours post-infection. PB2, PB1, HA, and NP vRNAs were analyzed using RT-qPCR analysis. Data represent the mean ±SD of two independent experiments, each performed in triplicate.

Figure 2
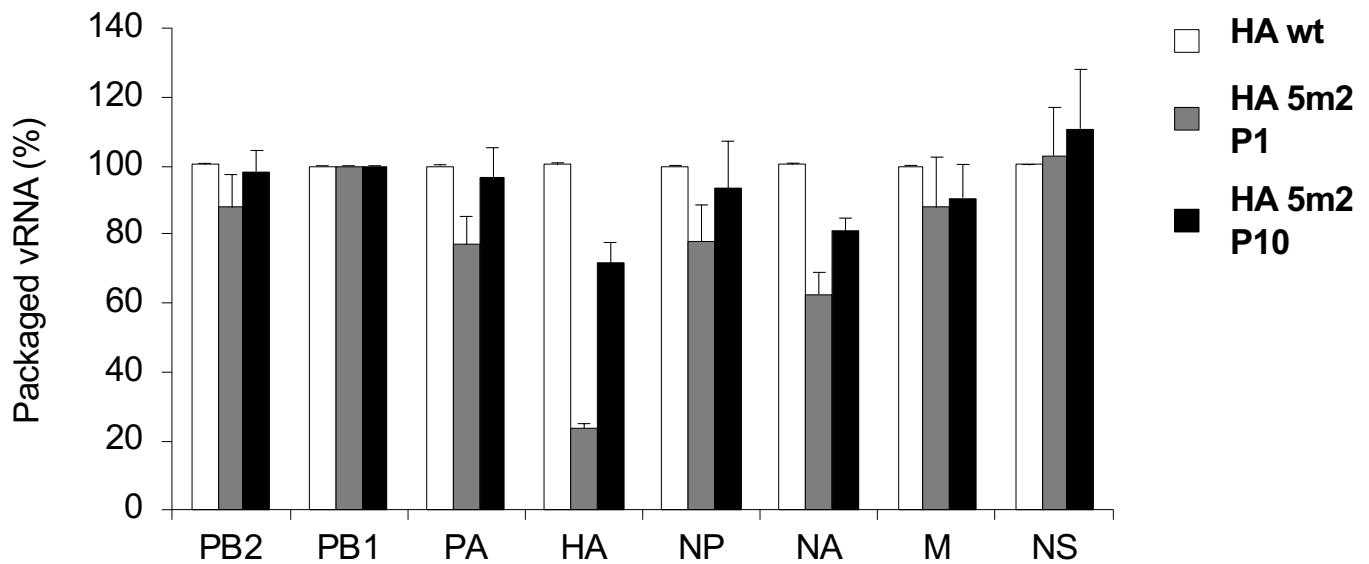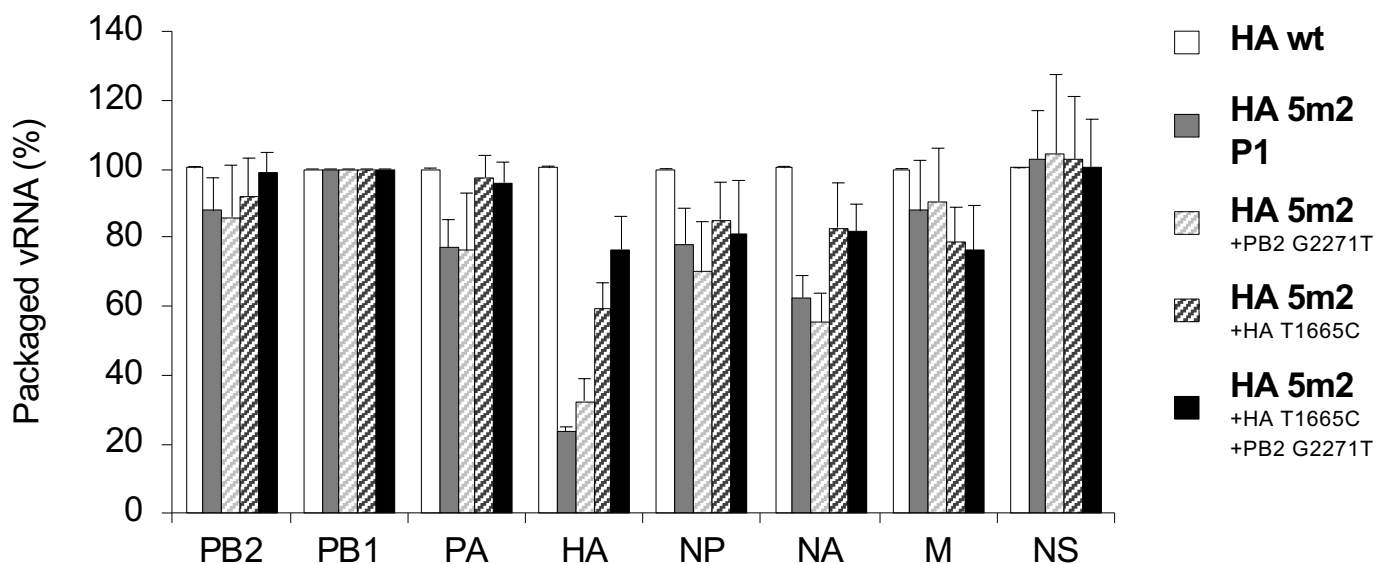
Fig 3. **Packaging of individual vRNA segments into progeny viral particles.** The amount of vRNA extracted from purified virus particles was quantified by RT-qPCR. All vRNAs were normalized to the amount of PB1 vRNA and to the average of that contained in the wild-type virus. Data represent the mean ±SD from two independent experiments each conducted in triplicate. (A) The panel shows the relative amounts of eight vRNA from the wild-type virus, HA 5m2 P10 virus, and HA 5m2 P1 virus. (B) The panel shows the relative amounts of eight vRNA from the wild-type virus and mutant HA 5m2 viruses.

Figure 3
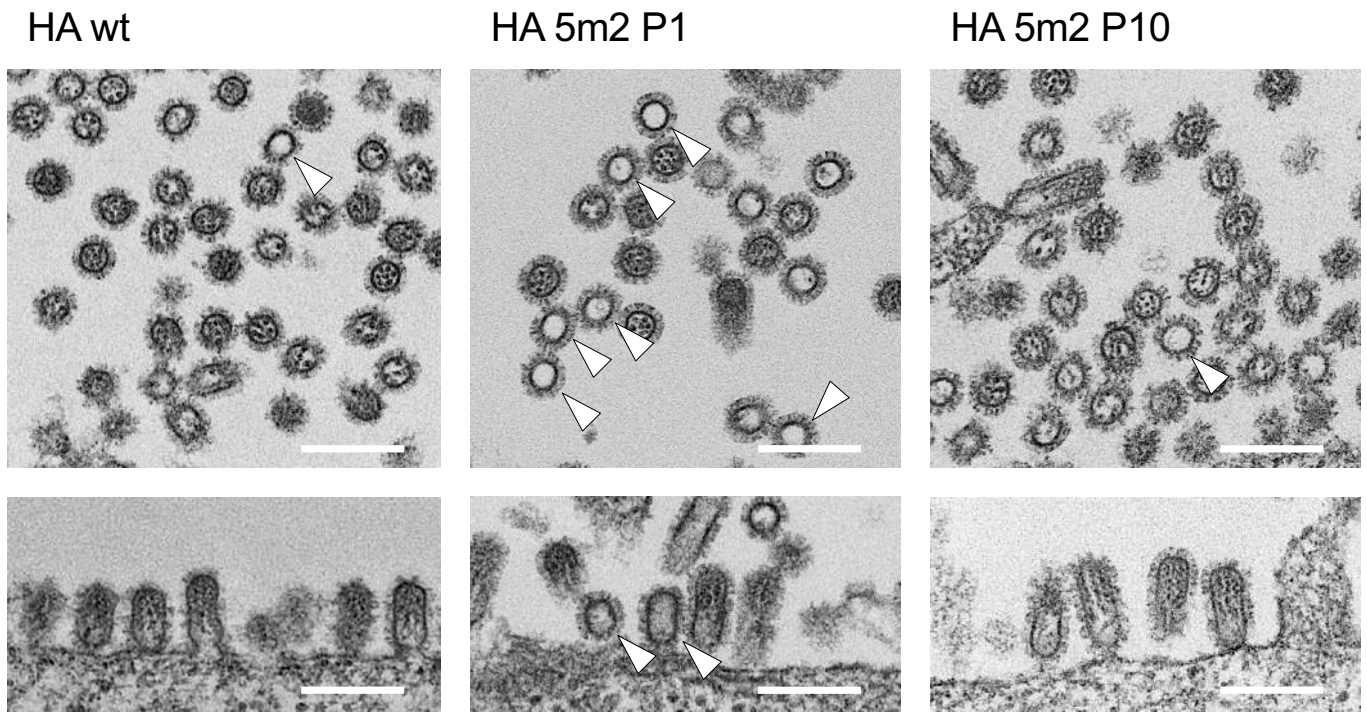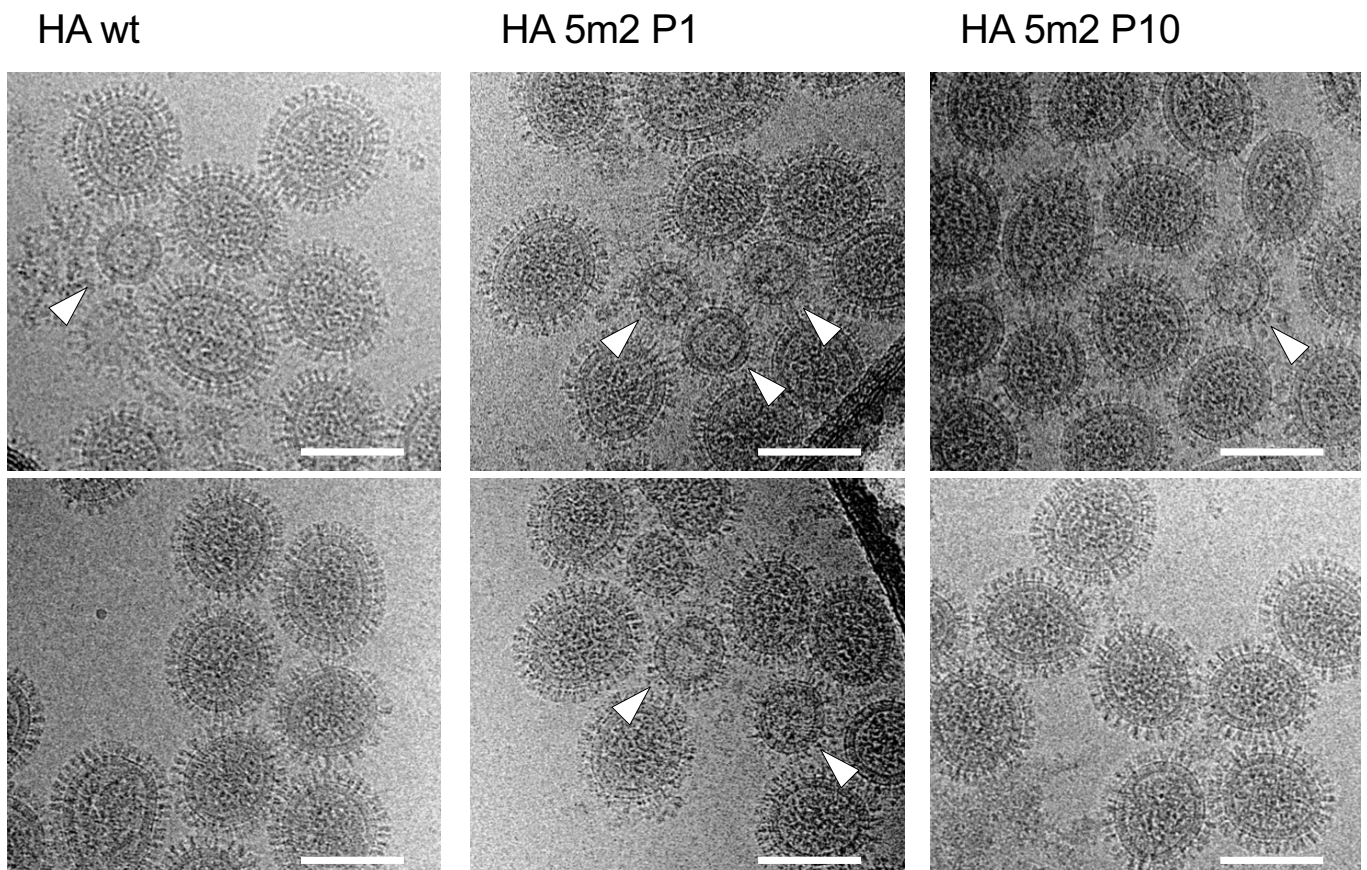
Fig 4. Morphology of HA 5m2 P1, HA5m2 P10, and wild-type viruses. (A) Ultrathin sections of viral particles budding from infected MDCK cells were observed using transverse section (upper side) and longitudinal section (lower side). Empty particles are indicated by arrowheads. Bars, 200 nm. (B) Purified virus particles were observed by cryo-TEM. Empty particles are indicated by arrowheads. Bars, 100 nm.
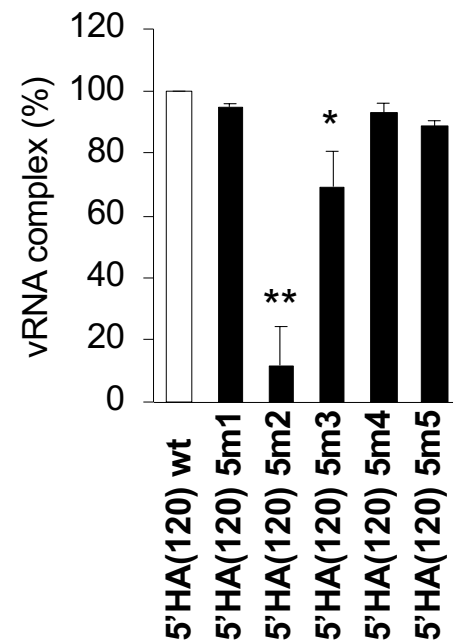
Figure 4
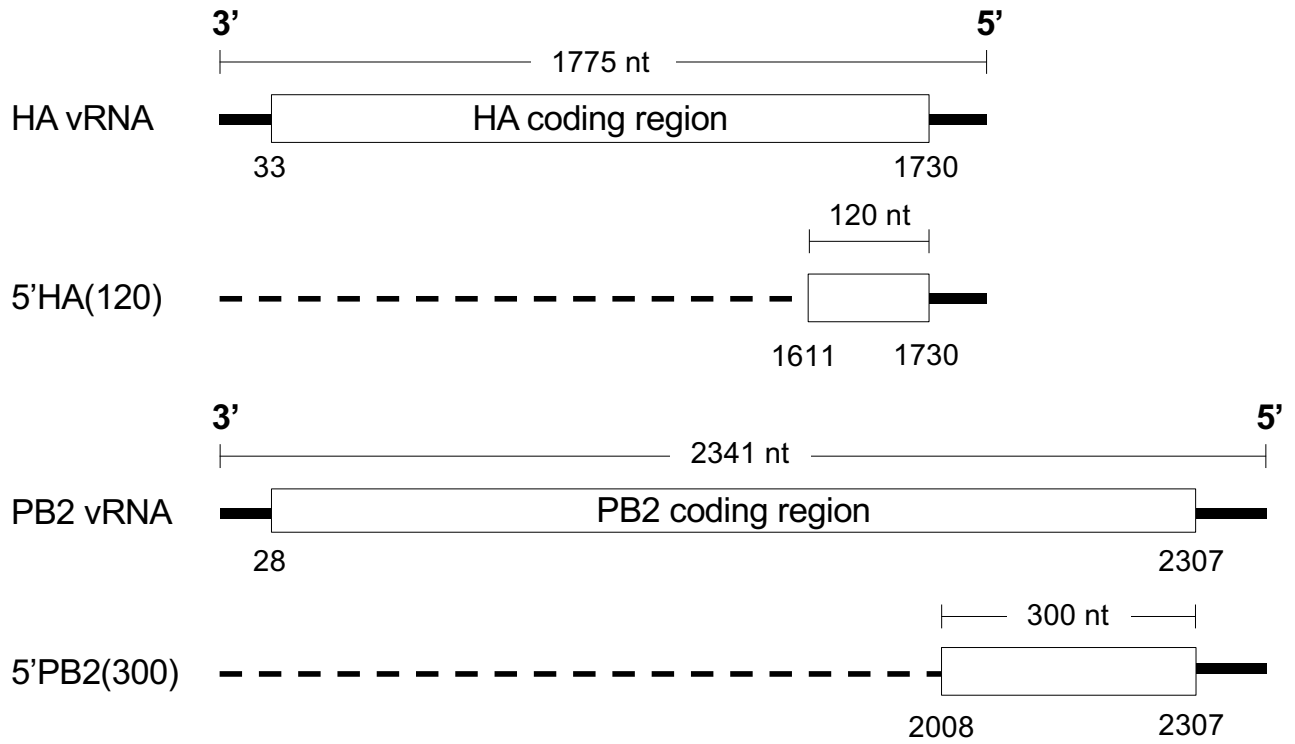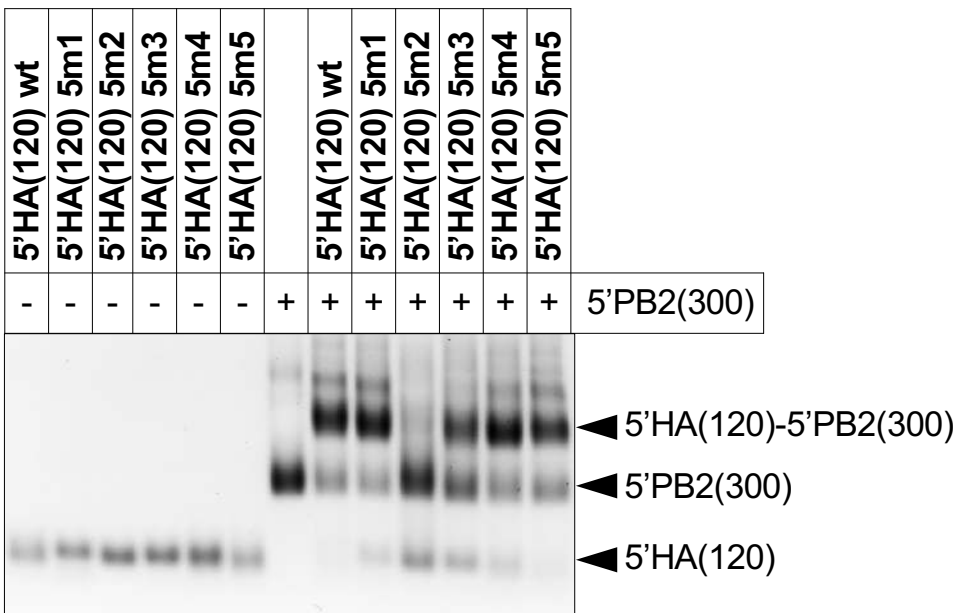
Fig 5. Gel shift assay using 5' end sequences of HA and PB2 vRNAs. (A) Schematic representation of 5'HA(120) and 5'PB2(300) vRNAs. The solid line represents the noncoding regions of vRNAs at the 3' and 5' ends. The white box represents the coding regions of the HA or PB2 proteins. The dashed line represents the deleted regions. 5'HA(120) and 5'PB2(300) contain 120 or 300 nucleotides in the coding and noncoding regions at their 5' ends, respectively. (B) The effect of silent mutations in 5'HA(120) vRNA on binding to 5'PB2(300) vRNA. 5'PB2(300) vRNA was incubated with wild-type and mutated 5'HA(120) vRNAs as indicated at the top of the gel image. Individual vRNA bands and vRNA complexes are indicated on the right. (C) Quantification of 5'HA(120)-5'PB2(300) complexes for each lane. The relative band intensity of the complex is indicated in comparison to that of the wild-type. The data represent the mean ± SD (n = 3). Dunnett's test; *P < 0.01; **P < 0.001.

Figure 5